

# Characterizing Absorption Spectrum of Natural Rubidium by Using a Directly Modulated VCSEL

Ido Ben-Aroya and Gadi Eisenstein

Department of Electrical Engineering, Technion, Haifa 32000, Israel  
bido@tx.technion.ac.il

**Abstract**—This paper describes a systematic procedure to select the optimum operating point of a directly modulated semiconductor laser which feeds a Rb based CPT system. The procedure is confirmed in a series of experiments.

## I. INTRODUCTION

Coherent Population Trapping (CPT) [1] is a phenomenon in which two hyperfine levels of the ground state in an atom are coupled by two coherent radiation fields to the same excited state ( $\Lambda$  configuration). This coupling leads to a drastic change in the excitation process and consequently in the populations of the system levels. The change in population can be related to a change in the absorption profile of a medium containing  $\Lambda$  system atoms. Moreover, the change leads to a very narrow resonance [2] which is the basis for a number of applications, including an atomic beam frequency standard (atomic clocks) [3].

The two coherent fields used for CPT are detuned relative to each other by the hyperfine splitting (HFS) frequency ( $f_{\text{hfs}}$ ). One technique to generate them is to use the two first order side bands of an amplitude modulated (AM) signal with the modulation frequency equaling  $f_{\text{hfs}} / 2$ . Namely, when using  $^{87}\text{Rb}$  vapor as the  $\Lambda$  system source, the two fields have to be generated from a signal at 780.24 nm which is modulated at 3.417 GHz.

Miniaturization of the system providing CPT resonances requires generation of the two optical fields from a compact source. Direct modulation of a nominally single longitudinal mode diode laser is an optimum solution enabling the required functionality together with compactness and low power consumption. Ideal conditions for CPT call for the first two AM side bands to have the same amplitudes. In practical lasers however, the side bands are somewhat asymmetric. The absolute need for single longitudinal mode operation calls for the use of either Distributed-Feedback (DFB) lasers (which are not commonly available at the wavelength ranges appropriate for Alkaline metals, commonly used as the media hosting  $\Lambda$  system) or Vertical Cavity Surface Emitting Lasers (VCSELs) which can operate at the required wavelengths. The modulation capabilities of

typical VCSELs exceed the required (few GHz) modulation frequency and hence, several compact CPT systems based on VCSELs have been reported [4-9].

Direct modulation of Semiconductor lasers is, however, non ideal. The finite linewidth enhancement factor (known as the  $\alpha$  parameter) [10] couples the real and imaginary parts of the susceptibility resulting in a degree of frequency modulation (FM) which inherently accompanies the AM. Moreover, the gain nonlinearity [11] together with the  $\alpha$  parameter yield a complex optical spectrum comprising high order side bands and an asymmetry in the amplitude of the first two side bands due to the so called Bogatov effect [12].

Implementation of CPT with a directly modulated VCSEL requires therefore an understanding of the interaction among two complex optical spectra: the VCSEL output and the absorption. Two modulation side bands, separated by  $f_{\text{hfs}}$  owe to coincide with the two relevant optical transitions in the  $\Lambda$  system. The DC operating point of the laser (which, together with the temperature, fine tunes the carrier wavelength) and the exact modulation frequencies are derived directly from the absorption spectrum of the atomic vapor. Identifying the correct spectral placing is a major task not possible without a detailed understanding of the interaction.

The absorption spectrum around the  $D_2$  line of Rb (780.24nm) contains peaks related to the two isotopes contained in the vapor,  $^{87}\text{Rb}$  and  $^{85}\text{Rb}$ . The interaction between the multi lobe absorption spectrum and the multi line modulated input allows for several possible CPT resonances and it is crucial to be able to choose the best in terms of contrast and width. In the more common case where only one isotope, say  $^{87}\text{Rb}$  is present in the vapor, the number of absorption peaks is halved but the complexity of the interaction with the laser spectrum is similar.

This paper addresses the details of a spectroscopic analysis of natural Rb ( $^{85}\text{Rb}$  and  $^{87}\text{Rb}$ ) where the absorption is probed by a directly modulated VCSEL. We discuss briefly the nonlinear modulation of the VCSEL. We present a model which interprets the interaction between the multi

line laser and absorption spectra and introduce a systematic algorithm for the identification of the optimum operating point. Finally we demonstrate CPT measurements of varying resonance quality which confirm the predictions of the model.

## II. VCSEL – RUBIDIUM OPTICAL INTERACTION

Understanding the absorption spectrum of natural Rb probed by a modulated VCSEL is crucial for choosing the correct operating point for CPT. This chapter describes the medium properties, the modulated VCSEL spectrum and the interaction between the VCSEL output and the vapor absorption spectrum.

### A. Absorption spectrum of natural Rubidium

Natural Rubidium consists of mainly two isotopes:  $^{85}\text{Rb}$  (72.2%) and  $^{87}\text{Rb}$  (27.8%). Focusing on the D<sub>2</sub> transition, both isotopes absorb around 780.24nm but their corresponding hyperfine splitting frequencies are different. The ground state of either isotope splits into two hyperfine levels detuned by an RF frequency. The excited state hyperfine splitting is masked by the  $\sim 500$  MHz Doppler broadening so that individual levels are indistinguishable by simple spectroscopy techniques. Thus, the expected transitions are: F=1,2→F' for  $^{87}\text{Rb}$  and F=2,3→F' for  $^{85}\text{Rb}$  with ground state hyperfine detunings of 6.834GHz and 3.035GHz, respectively.

The experimental setup used in the experiments we report comprises a temperature controlled; single mode VCSEL driven by a low-noise DC current source and emitting near 780 nm. The DC bias serves to control the output power and wavelength. A current increase lengthens the emitted wavelength since thermal rather than pure carrier effects [13] dominate the operation of the present VCSEL.

At a temperature of 16.2°C and a bias of 1.4 mA, the VCSEL emitted in a single wavelength around 780.24nm and in a well controlled single spatial mode. The VCSEL output was collimated into a 5mm diameter beam and its polarization was set to be circular. The collimated beam impinges on the input port of a 26mm diameter cylindrical glass cell with a length of 48mm. The cell contained natural Rb vapor (with no buffer gas) at a temperature of 34.4°C which provided peak absorption of nearly 50%. The transmitted power was detected by a large area ( $1\text{cm}^2$ ) silicon detector.

The measured transmitted intensity for different VCSEL bias levels (near 1.4 mA) is shown in Fig. 1a. The spectrum contains four peaks as expected. Since the bias changes the wavelength and power, the overall curve exhibits a linear increase. This is an artifact which can be easily compensated for mathematically, as shown in Fig. 1b. In Fig. 1b we also translate the bias changes into frequency shifts, yielding the absorption profile of the medium.

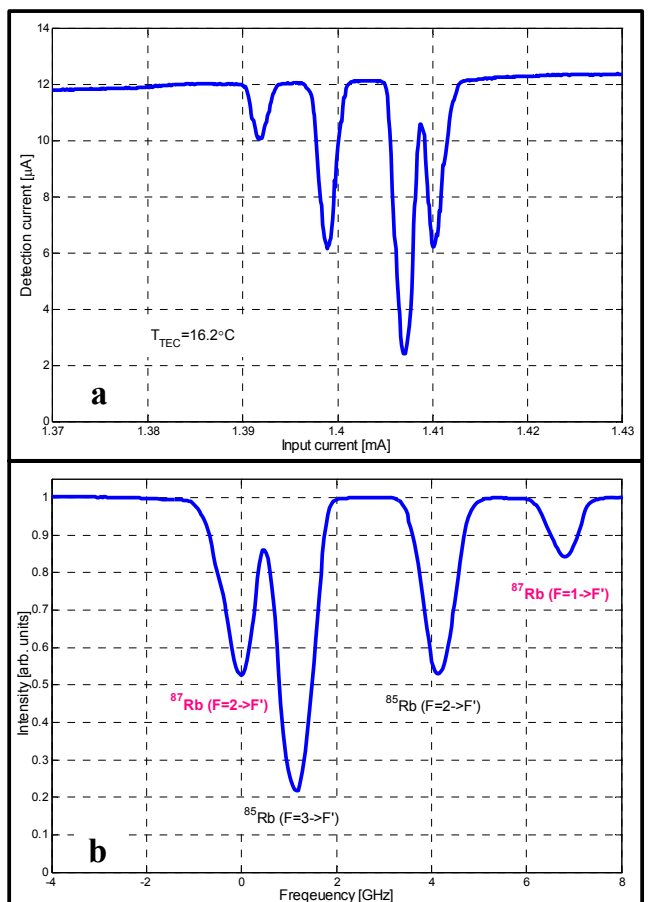


Figure 1. Absorption spectra of natural Rb. (a) Bias dependent absorption. (b) Optical frequency dependent spectrum, compensated for bias dependent VCSEL power changes.

### B. Optical spectrum of the directly modulated VCSEL

The optical spectrum of the directly modulated VCSEL differs significantly from an ideal AM spectrum as seen schematically in Fig. 2. Three features, each signifying a specific physical parameter or processes are apparent. First, the first two sidebands, separated from the carrier by the modulation frequency  $f_{\text{hs}}/2$  have unequal amplitudes. This asymmetry stems from the Bogatov effect [12] and increases for larger  $\alpha$  parameters. Second, the laser nonlinearity generates harmonics of these side bands. Since the nonlinearity is complex and frequency dependent, the amplitudes of the harmonics have a complicated distribution which is strongly dependent on the RF power level. An increase in RF power causes therefore several simultaneous effects: a larger modulated optical component, a change in the relative power among the many lines and a spectral shift of the entire comb towards longer wavelengths (due to heating). Finally, the finite  $\alpha$  parameters and the consequent induced chirp [13] broaden the linewidth of each spectral line. However, the linewidth is much narrower than the separation between lines.

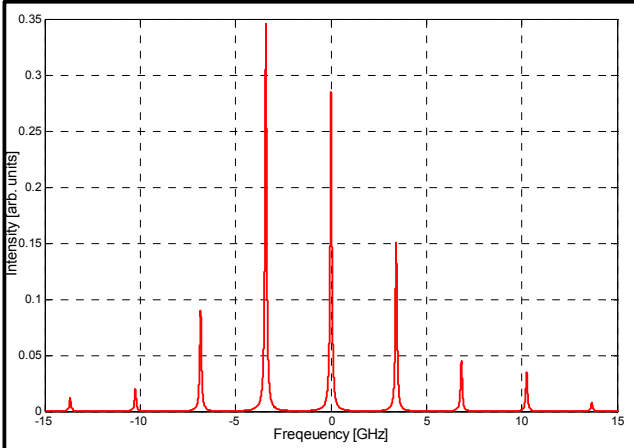


Figure 2. Schematic spectrum of a directly modulated VCSEL. The modulation frequency is  $f_{\text{hfs}} / 2 = 3.417341 \text{ GHz}$ .

### C. Absorption spectrum of natural Rb probed by a modulated VCSEL

The CPT process requires that two coherent fields induce simultaneously two transitions; from the hyperfine split ground states to the single excited state. The optical spectrum of the modulated VCSEL comprises a comb of narrow lines with several pairs having a spectral separation of  $f_{\text{hfs}}$ . Varying the DC bias over a moderate range, while keeping the RF power constant, amounts to spectrally scanning the entire comb of lines (Fig. 2). The scanning comb interacts with the Rb vapor so that the spectrum at the Rb cell output represents the interaction between modulated VCSEL comb and the Rb absorption spectrum. Whenever two spectral lines overlap the two transitions defined by the  $\Lambda$  configuration, CPT is, in principle, obtainable and the corresponding DC bias is a suitable operation point.

The measured absorption spectrum of natural Rb probed by a modulated VCSEL is shown in Fig. 3a. The modulation frequency was  $f_{\text{hfs}} / 2$  for  $^{87}\text{Rb}$  namely, 3.417341GHz and the RF power was +2.0dBm. Since the frequency is scanned using the DC bias, the signal experience also a linear increase in intensity which is easily compensated. Note that the RF power changes both the output level and the wavelength, compared to the case shown in Fig. 1.

Fig. 3b describes the same measurement as Fig. 3a except that the bias axis was replaced with the corresponding optical frequency and the DC tilt was corrected for. The spectrum includes several peaks resulting from the complicated interaction of the comb and the four peaks of the Rb absorption profile. The model presented in section III below analyzes the various peaks and identifies the proper peak to be locked so as to obtain the best CPT resonance.

### III. THE INTERACTION MODEL

The interaction we are modeling (Fig. 3) is, of course, highly nonlinear. We use a small signal linearized approach where the two spectra are convoluted linearly. The output spectrum is interpreted in three steps:

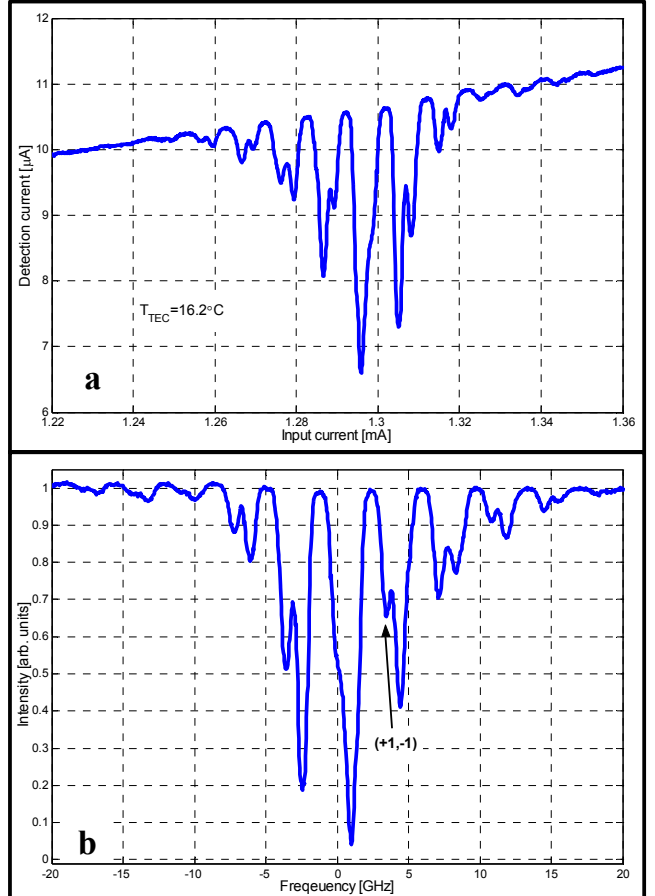


Figure 3. Absorption spectra of natural Rb probed by a modulated VCSEL. (a) Bias dependent absorption. (b) Optical frequency dependent spectrum, compensated for bias dependent VCSEL power changes. The minimum point  $(+1, -1)$ , results from the interaction of the first two side lobes with the  $^{87}\text{Rb}$  transition.

- Shifting the medium absorption spectrum by multiples of the RF drive frequency.
- Weighting the shifted peaks by the power distribution of the diode spectral lines.
- Adding the resulting contributions linearly.

First we describe the VCSEL optical spectrum as a comb of a finite number of delta functions placed in the spectral vicinity of the carrier frequency. At this stage, the delta functions have equal amplitudes and are shifted from each other by the modulation frequency. Every delta function is replaced next by the absorption spectrum of the medium. If the modulation frequency equals to the appropriate HFS frequency multiplied by  $1/m$ , where  $m$  is a natural number, there is a point in the spectrum in which the two transitions related to the CPT process coincide.

Defining  $i$  and  $j$  as integers representing two of the comb lines (where  $i = 0$  represents the carrier), yields  $|i - j| = m$  if and only if  $i$  and  $j$  represent two different lines in the comb corresponding to two absorption profiles which overlap exactly at the absorption peaks related to the corresponding

transitions in the  $\Lambda$  system. For example, Modulating the laser by half the HFS frequency of  $^{87}\text{Rb}$  provides potential operation points suitable for CPT in every place in the spectrum where two absorption peaks related to the  $^{87}\text{Rb}$   $F=1 \rightarrow F'$  and  $F=2 \rightarrow F'$  transitions, derived from different lobes, overlap. The frequency deviation between those lobes is precisely  $f_{\text{hfs}}$ .

Figure 4 shows a measured absorption spectrum of natural Rb relative to a few comb lines obtained by modulating VCSEL at  $f_{\text{hfs}} / 2$ . The marker ‘a’ indicates an operation point in which the  $^{87}\text{Rb}$   $F=1 \rightarrow F'$  and the  $^{87}\text{Rb}$   $F=2 \rightarrow F'$  transitions related to the +1 (blue dashed line) and -1 (red dotted line) lobes, respectively, are matched.

The Second step of the model deals with the unequal amplitudes of the lines in the VCSEL spectral comb. This distribution is accounted for by properly weighting the lines which were replaced with the absorption spectrum comb of the medium (in the first step) according to the RF modulated spectral power distribution.

The weighting function considers the weight of each line,  $w_i$ , keeping  $\sum w_i = 1$ . The function can be found by measuring the spectral power lines or by deriving it from the measured spectrum (Fig. 3). Direct high resolution measurements of the spectral power distribution (usually obtained using a Fabry-Perot interferometer) yield only, in most cases, low order side bands. Although the carrier and the first side bands comprise most of the emitted power, important information is contained in the interactions of the high order side bands.

The second procedure extracts the weight function of all lines from the measured spectrum. The combined contributions from all weighted and shifted absorption spectral lines yield, through an optimization procedure, a spectrum which is identical to the measured one. However, inaccuracies prevent the exclusive use of standard techniques such as Min Mean Square Error (MMSE) or Minimum Mean Distance Error (MMDE) and manual tuning had to be added.

The most accurate spectral distributions are obtained by combining an interferometer measurement and the extraction procedure. Fig 5 demonstrates a so determined weight function which matches the measured spectrum of Fig. 3. The wavelength and output level shift due to the RF addition was compensated for in Fig. 5 for comparison.

The match between the measured and extracted spectra serves to identify the peaks of Fig. 5, one at a time. Each peak originates from one or more transitions in the natural Rb, due to the interaction with the spectral comb. The transitions responsible for each one of the peaks is found by investigating the shifted absorption spectra presented in Fig. 4.

The identification procedure can also be implemented in a reversed order. The desired transitions are defined first and the absorption spectrum lobes which overlap them are consequently easily identified. The goal of the procedure is to determine particular DC bias levels where the overlap

takes place. For example, CPT of  $^{87}\text{Rb}$  can be observed using the first two side lobes ( $i=+1$  and  $j=-1$ ) of a VCSEL which is modulated at half the HFS frequency. The overlap of the  $^{87}\text{Rb}$   $F=1 \rightarrow F'$  and  $F=2 \rightarrow F'$  transitions is marked in Fig. 4 by ‘a’. The corresponding DC bias levels are those that yield a minimum in the vapor spectrum (when probed by the modulated VCSEL) and are termed proper operating points.

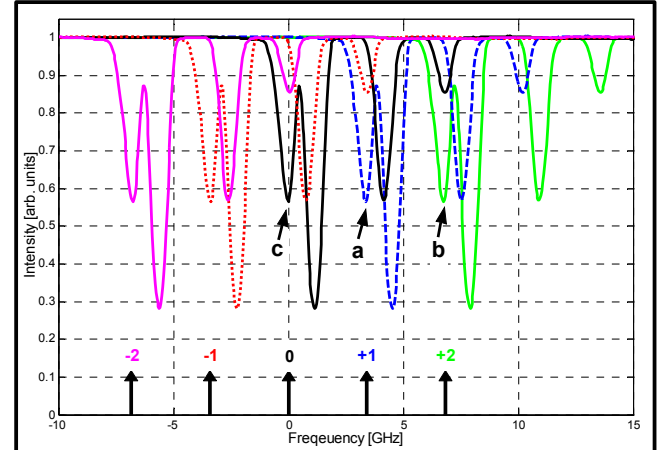


Figure 4. Shifted interaction spectra placed against several, near center, comb lines. The point marked **a** represents the  $(+1; -1)$  operating point, the point **b** belongs to  $(+2; 0)$  and **c** is for  $(0; -2)$ . The numbers count the lobes with **0** being the carrier.

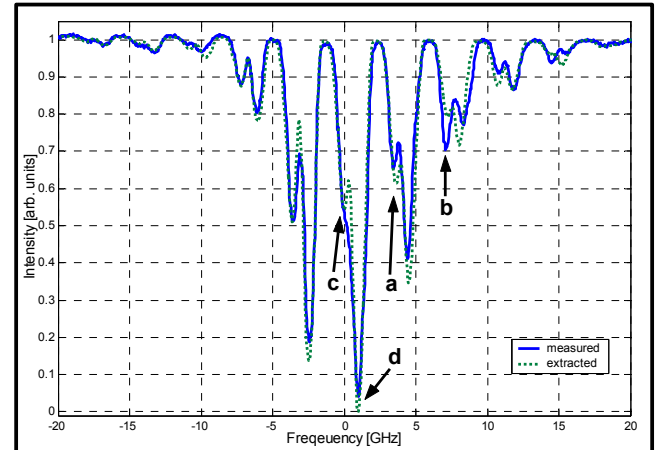


Figure 5. Measured spectrum (blue) compared to the spectrum extracted using the model (dotted green). The weighting function which was used is:  $w_0 = 0.285$ ,  $w_1 = 0.150$ ,  $w_{-1} = 0.345$ ,  $w_2 = 0.045$ ,  $w_{-2} = 0.090$ ,  $w_3 = 0.035$ ,  $w_{-3} = 0.020$ ,  $w_4 = 0.008$ ,  $w_{-4} = 0.012$  and  $w_{-5} = 0.010$ . The points **a**, **b** and **c** are for the same operating points as in Fig. 4. Point **d** is related to  $^{85}\text{Rb}$  transitions.

#### IV. MEASUREMENTS OF CPT RESONANCES

The analysis presented in chapter III predicts a number of suitable operating points for the observation of the CPT process in  $^{87}\text{Rb}$ . Each operating point is related to a different pair of lobes interacting with the vapor. The modulating frequency and power of the diode were (as before)  $f_{\text{hfs}} / 2$  and +2.0dBm, respectively. The modulation frequency initiates the use of two lines in the comb for which  $| i - j | = 2$ . These

are for example: (+2;0), (+1;-1), (0;-2), etc... Moreover, the experiment requires that a minimum point in the spectrum be locked in order to stabilize the VCSEL.

Measurements of CPT 0-0 resonances obtained for the operating points (+1;-1) and (+2;0) are presented in Fig. 6 and 7, respectively. Due to some inaccuracies in the model, the minimum at the point (0;-2), which can also serve as a proper point is masked to a degree which prevents the system from locking. The (0;-2) operating point emerges as a clear minimum when the RF power to the VCSEL is reduced to 0dBm. Under those conditions, a CPT 0-0 resonance is observable at (0;-2) as shown in Fig 8. The asymmetry in Fig. 8 results from the FM spectroscopy technique used for measuring CPT: The large  $\alpha$  parameter of the diode gives rise to an additional AM modulation which distorts the measurement [14-17].

Locking the system to a minimum point not satisfying  $|i - j| = 2$  yields no CPT resonance. For example, the strongest peak marked with 'd' in Fig. 5 is inappropriate and can not be used for  $^{87}\text{Rb}$  CPT measurements. Attempts to lock on this point yield only noise as seen in Fig. 9. Using Fig. 4 it is easy to determine that this point is related to  $^{85}\text{Rb}$  rather than  $^{87}\text{Rb}$ .

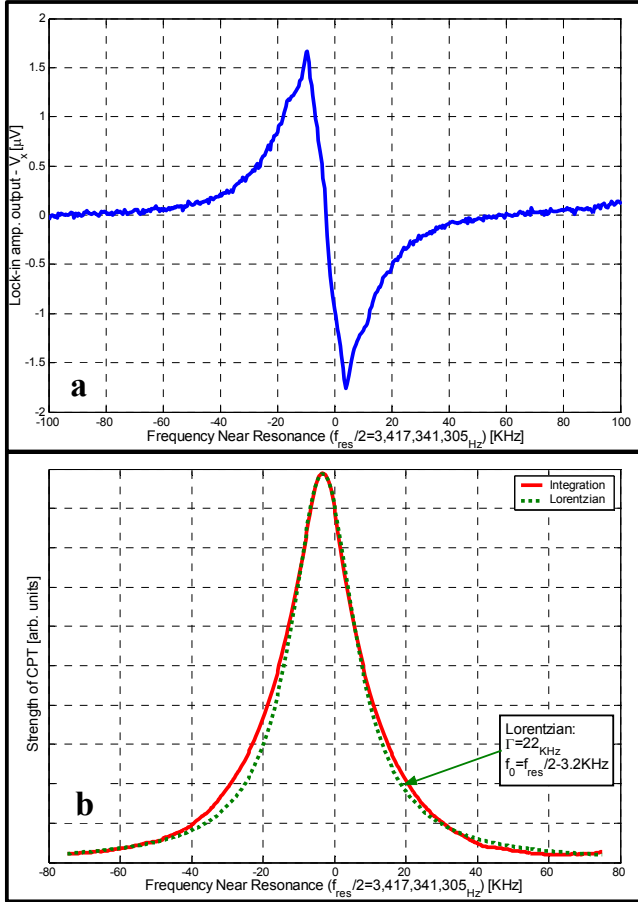


Figure 6. CPT 0-0 resonance measurement of  $^{87}\text{Rb}$  D<sub>2</sub> line, at the point (+1; -1). (a) Raw data representing the derivative of the actual resonance. (b) Integration of the measurement in (a) and its fit to a Lorenzian.

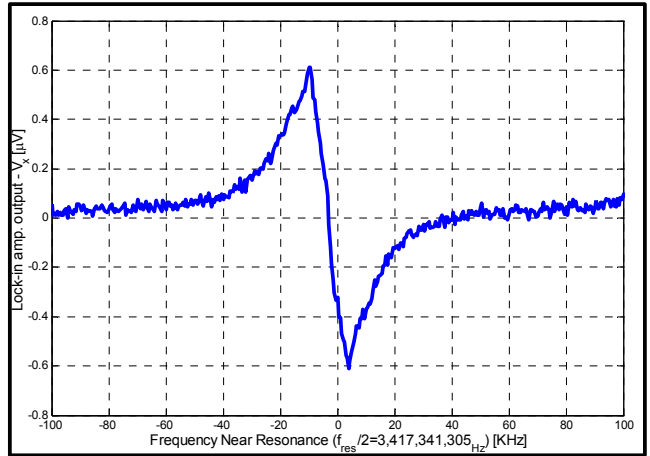


Figure 7. Measured derivative of the CPT 0-0 resonance of  $^{87}\text{Rb}$  D<sub>2</sub> line, at the point (+2; 0).

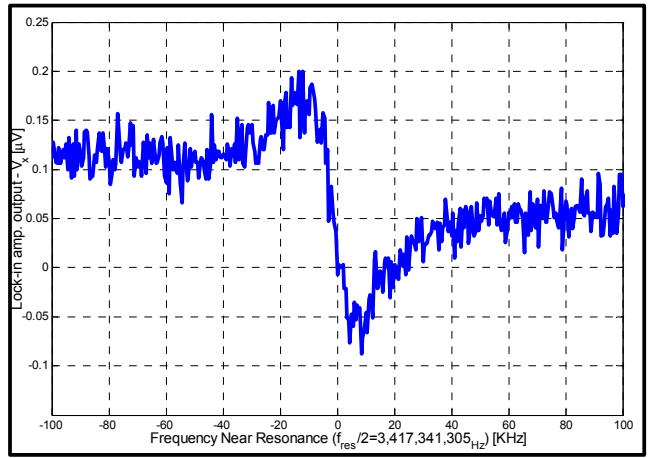


Figure 8. Measured derivative of the CPT 0-0 resonance of  $^{87}\text{Rb}$  D<sub>2</sub> line, at the point (0; -2).

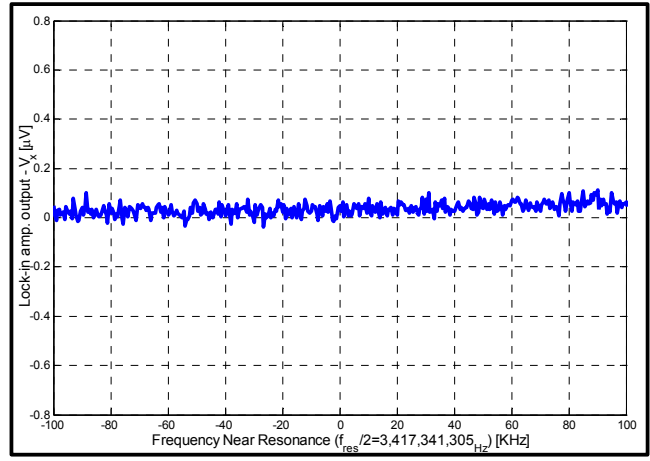


Figure 9. CPT measurement attempt at the point d of Fig. 5.

## V. CONCLUSIONS

This paper described a systematic procedure to select a proper operating point of a modulated VCSEL which feeds a natural Rb CPT system. The interaction among two multi lobe complicated spectra; of the modulated VCSEL and the Rb absorption, is treated as a linear convolution. The result is a spectrum comprising very many minima but the procedure enables to distinguish those which are suitable for CPT. The procedure was confirmed experimentally by a series of measurements of CPT resonances in  $^{87}\text{Rb}$  hosted by a natural Rb vapor cell.

The same mechanism can be used to select CPT conditions for  $^{85}\text{Rb}$ . In that case, the resonance is at 3.03573GHz and the absorption change is likely to be stronger [18]. Hence, demonstrating CPT with  $^{85}\text{Rb}$  is simpler. Moreover, if a single isotope is used, the absorption spectrum is, of course, simpler and the entire observed minima enable, in principle, CPT. Nevertheless, the available resonances are not identical and it is crucial to be able to pick the optimum point.

Most practical systems contain a buffer gas which broadens the absorption spectrum of the medium. Too large of a gas pressure may broaden the spectrum to a degree which masks the individual lines resulting from the interaction with the modulated VCSEL.

Finally, the peak identification process we presented may serve to solve the important problem of CPT based systems turn on. The scheme we propose can be easily automated to always lock on the same, optimal absorption peak.

## ACKNOWLEDGMENT

This work was partially supported by Accubeat Inc. and the Israeli ministry of defense within a project to develop a chip scale atomic clock. The authors acknowledge Dr. A. Stern of Accubeat Inc. and Prof. M. Rosenblu of Bar Ilan University for fruitful discussions and technical help.

## REFERENCES

- [1] E. Arimondo, "Coherent population trapping in laser spectroscopy", in *Progress in Optics*, vol. XXXV, Edited by E. Wolf, North Holland 1996, pp. 257-354.
- [2] R. Wynands and A. Nagel, "Precision spectroscopy with coherent dark states", *Appl. Phys. B*, vol. 68, pp. 1-25, 1999.
- [3] N. Cyr, M. Têtu and M. Breton, "All-optical microwave standard: aproposal", *IEEE Trans. Instrum. Meas.*, vol. 42, no. 2, pp. 640-649, April 1993.
- [4] C. Affolderbach, A. Nagel, S. Knappe, C. Jung, D. Wiedenmann and R. Wynands, "Nonlinear spectroscopy with a vertical-cavity surface-emitting laser (VCSEL)", *Appl. Phys. B*, vol. 70, pp. 407-417, 2000.
- [5] J. Kitching, S. Knappe, N. Vukičević, L. Hollberg and W. Weidmann, "A microwave frequency reference based on VCSEL-driven dark line resonance in Cs vapor", *IEEE Trans. Instrum. Meas.*, vol. 49, no. 6, pp. 1313-1317, December 2000.
- [6] R. Lutwak, D. Emmons, W. Riley and R. M. Garvey, "The chip-scale atomic clock-coherent population trapping vs. conventional interrogation", in *Proceedings of the 34<sup>th</sup> annual precise time and time interval (PTTI) systems and applications meeting*, December 2002, pp. 539-550.
- [7] S. Knappe, V. Shah, P. D. D. Schwindt, L. Hollberg and J. Kitching, "A microfabricated atomic clock", *Appl. Phys. Lett.*, vol. 85, no. 9, pp. 1460-1462, August 2004.
- [8] S. Knappe, P. D. D. Schwindt, V. Shah, L. Hollberg and J. Kitching, "A chip-scale atomic clock based on  $^{87}\text{Rb}$  with improved frequency stability", *Optics Express*, vol. 13, no. 4, pp. 1249-1253, February 2005.
- [9] P. D. D. Schwindt, S. Knappe, V. Shah, L. Hollberg, J. Kitching, L. A. Liew and J. Moreland, "Chip-scale atomic magnetometer" *Appl. Phys. Lett.*, vol. 85, no. 26, pp. 6409-6411, December 2004.
- [10] C. H. Henry, "Theory of the linewidth of semiconductor lasers", *IEEE J. Quantum Electron.*, vol. QE-18, no. 2, pp. 259-264, February 1982.
- [11] R. Olshinsky, P. Hill, V. Lanzisera, W. Powazinik, "Frequency response of  $1.3\ \mu\text{m}$  InGaAsP high speed semiconductor lasers", *IEEE J. Quantum Electron.*, vol. QE-23, no. 9, pp. 1410-1418, September 1987.
- [12] A. P. Bogatov, P. G. Eliseev and B. N. Svedlov, "Anomalous interaction of spectral modes in a semiconductor laser", *IEEE J. Quantum Electron.*, vol. QE-11, no. 7, pp. 510-515, July 1975.
- [13] N. K. Dutta, N. A. Olsson, L. A. Koszi, P. Besomi, R. B. Wilson, and R. J. Nelson, "Frequency chirp under current modulation in InGaAsP injection lasers", *J. Appl. Phys.*, vol. 56, no. 7, pp. 2167-2169, October 1984.
- [14] G. C. Bjorklund, M. D. Levenson, W. Length and C. Ortaiz, "Frequency modulation (FM) spectroscopy – theory of lineshapes and signal-to-noise analysis", *Appl. Phys. B*, vol 32, pp. 145-152, 1983.
- [15] W. Length, "High frequency heterodyne spectroscopy with current-modulated diode laser", *IEEE J. Quantum Electron.*, vol. QE-20, no. 9, pp. 1045-1050, September 1984.
- [16] M. Gehretz, G. C. Bjorklund and E. A. Whittaker, "Quantum-limited laser frequency-modulation spectroscopy", *J. Opt. Soc. Am. B*, vol. 2, no. 9, pp. 1510-1526, September 1985.
- [17] R. Wynands and A. Nagel, "Inversion of frequency-modulation spectroscopy line shapes", *J. Opt. Soc. Am. B*, vol. 16, no. 10, pp. 1617-1621, October 1999.
- [18] M. Stähler, R. Wynands, S. Knappe, J. Kitching, L. Hollberg, A. Taichenachev and V. Yudin, "Coherent population trapping resonances in thermal  $^{85}\text{Rb}$  vapor:  $D_1$  versus  $D_2$  line excitation", *Opt. Lett.*, vol. 27, no. 16, pp. 1472-1474, August 2002.